

Theoretical and experimental investigation of the light shift in Ramsey-CPT

Wujie Gao, Yuichiro Yano,* and Shigeyoshi Goka

*Graduate School of Science and Engineering, Tokyo Metropolitan University,
Minami-Osawa, Hachioji, Tokyo 192-0397, Japan*

Masatoshi Kajita

*National Institute of Information and Communications
Technology, Koganei, Tokyo 184-8795, Japan*

(Date textdate; Received textdate; Revised textdate; Accepted textdate; Published textdate)

Abstract

We theoretically and experimentally investigated the light shift (AC Stark shift) of the $6^2S_{1/2}$ ($F = 3 \leftrightarrow 4$) transition frequency in ^{133}Cs , as observed through coherent population trapping (CPT) using a pulsed laser light. There is a good agreement between the calculation and experiment proving the dependence of the light shift on various pulsed laser parameters. The dependence of the light shift on the laser intensity is non-linear at a small intensity. However, it is linear at a higher intensity, and the theoretical slope is 50 times lower than that when using continuous excitation. We then investigated the effect of the observation timing of the resonance signal on the light shift. We found in the observation during an early time that the shift is small.

*Electronic address: yano-yuichiro@ed.tmu.ac.jp

I. INTRODUCTION

Compact atomic clocks are required for many applications fields such as in telecommunications, navigation systems, and synchronization of networks [1]. Atomic clocks based on coherent population trapping (CPT) have attracted much attention as fabricating compact frequency references [2]. In general, atomic clocks are demanded for long term frequency stability. Long term frequency instability is caused by frequency shifts due to changes in the measurement conditions.

It is well known that the buffer gas and light shifts in CPT atomic clocks are limiting factors of long term stability [3]. The buffer gas is often contained in the gas cell in order to suppress the relaxation of atoms due to collisions between them and the vapor cell wall, which is important for observing the narrow resonance linewidth; However, the frequency shift is caused by and depends on the vapor pressure and the temperature of the gas cell [4]. Fortunately, the way to combine two buffer gases that have frequency shifts in opposite directions to the temperature have been reported on to reduce temperature dependence [5, 6], and this allows for a good temperature coefficient of frequency (TCF) to be obtained. In addition, zero TCF is observed in the 70 to 80 °C range by using Ne buffer gas [7]. The light shift is the frequency shift depending on the light intensity incident on the atoms. The light shift under a continuous wave proportionally increases with the increase in light intensity. The frequency sensitivity to the light intensity is higher than that to the temperature. Therefore, the light shift is a dominant factor limiting the long term stability of CPT atomic clocks [8].

Several methods have been proposed for suppressing the light shift [9–11]. In particular, it has previously been reported that the Raman-Ramsey scheme significantly suppresses the light shift [12–14]. As a result, a high frequency stability of $2 \sim 3 \times 10^{-14}$ at 200 s can be obtained using a Cs vapor cell [15]. However, the relation between the light shift and the interrogation parameters is still unclear. Therefore, it is necessary to investigate the relation between the light shift and the interrogation parameters, such as the light intensity, free evolution time, and observation timing, in order to enhance the long term frequency stability.

We theoretically and experimentally investigated the light shift of the $6^2S_{1/2}$ ($F = 3 \leftrightarrow 4$) transition frequency in ^{133}Cs under pulse excitation for this paper. The light shift in Ramsey-

CPT is calculated based on a density matrix analysis. We also show the experimental results using a ^{133}Cs gas cell and the D_1 -line VCSEL. The calculated and measured light shift as a function of the total light intensity is also shown. The results showed that the light shift under pulse excitation is significantly less than that under continuous excitation. In addition, the light shift is non-linear at a small intensity. We also show the light shift as a function of the observation timing, which shows that the light shift under pulse excitation is dependent on the observation timing and increases with the increase in observation timing. We also made an observation during the early stages and noted the shift was small. Since these results show there is a good agreement between the calculation and experiment proving the dependence of the light shift on various pulsed laser parameters, we now know that the analytical method gives us a precise estimation of the light shift with a Ramsey-CPT resonance.

II. THEORY

Figure 1 (a) shows the excitation scheme using a left circular (σ^+) polarized light field on the ^{133}Cs - D_1 line. In the CPT phenomenon, two-ground states of the $6^2S_{1/2}$ are coupled to common excited state of the $6^2P_{1/2}$, simultaneously.

In this system, the dynamical behavior of the density matrix ρ is governed by the quantum Liouville equation,

$$\frac{\partial}{\partial t}\rho(t) = \frac{i}{\hbar}[\rho, H] + R\rho, \quad (1)$$

where H is the Hamiltonian matrix for this three level system and R stands for the relaxation terms. Using the rotating wave approximation with the simplified Λ -type model shown in Fig. 1 (b), Eq.(1) can then be rewritten as

$$\begin{aligned}
\dot{\rho}_{11} &= i\frac{\Omega_p}{2}(-\rho_{13} + \rho_{31}) + \Gamma_{31}\rho_{33} + \gamma_s(\rho_{22} - \rho_{11}) \\
\dot{\rho}_{22} &= i\frac{\Omega_c}{2}(-\rho_{23} + \rho_{32}) + \Gamma_{32}\rho_{33} - \gamma_s(\rho_{22} - \rho_{11}) \\
\dot{\rho}_{33} &= i\frac{\Omega_p}{2}(\rho_{13} - \rho_{31}) + i\frac{\Omega_c}{2}(\rho_{23} - \rho_{32}) - \Gamma_3\rho_{33} \\
\dot{\rho}_{12} &= i\rho_{12}(\delta_p - \delta_c) - i\frac{\Omega_c}{2}\rho_{13} + i\frac{\Omega_p}{2}\rho_{32} - \gamma_s\rho_{12} \\
\dot{\rho}_{13} &= i\rho_{13}\delta_p - i\frac{\Omega_c}{2}\rho_{12} + i\frac{\Omega_p}{2}(\rho_{33} - \rho_{11}) - \gamma_f\rho_{13} \\
\dot{\rho}_{23} &= i\rho_{23}\delta_c - i\frac{\Omega_p}{2}\rho_{21} + i\frac{\Omega_c}{2}(\rho_{33} - \rho_{22}) - \gamma_f\rho_{23}
\end{aligned} \tag{2}$$

and the density matrix trace satisfies the closed system condition.

$$\text{Tr}(\rho) = \rho_{11} + \rho_{22} + \rho_{33} = 1 \tag{3}$$

Here, $|1\rangle$ and $|2\rangle$ correspond to the two ground states $|F = 3, m_F = 0\rangle$ and $|F = 4, m_F = 0\rangle$ in the $6^2S_{1/2}$ state, and the $|3\rangle$ corresponds to $6^2P_{1/2}$.

The total emission rate is $\Gamma_3 = \Gamma_{31} + \Gamma_{32}$, and $\Gamma_{31} = \Gamma_{32}$, $\gamma_f = \Gamma_3/2$, γ_s is a minuscule quantity $\gamma_s \ll \gamma_f$ for the case where the cell does not contain a buffer gas [16]. In the case of bichromatic light, we have the relation: $\delta_p = -\delta_c = \Delta_0/2$.

Figure 2 shows the Ramsey interrogation sequence [17]. The first laser pulse of duration τ irradiates the atoms into the dark state. After a free evolution time T , the same laser irradiates the atoms again. Immediately after a pulse rise, the transmitted intensity of the second pulse is measured at the end of τ_o and the atoms are prepared for the next measurement. This pulse cycle is repeatedly executed until the atomic state reaches equilibrium. The Rabi frequency in this scheme is expressed as

$$\begin{cases} \Omega_p, \Omega_c > 0 & (0 < t < \tau) \\ \Omega_p = \Omega_c = 0 & (\tau < t < \tau + T) \end{cases} \tag{4}$$

Since the Liouville equation does not contain the frequency shift term with regard to the light intensity, and the light field will shift the energy levels of the two ground states via the light shift, we include the light shift terms in Eq. (2).

$$\begin{aligned}
\delta_p &= \frac{\Delta_0}{2} + LS_1\left(\frac{\Delta_0}{2}, \Omega_p\right) \\
\delta_c &= -\frac{\Delta_0}{2} + LS_2\left(-\frac{\Delta_0}{2}, \Omega_c\right)
\end{aligned} \tag{5}$$

where LS_1 and LS_2 are the light shifts under continuous excitation. These light shift terms are the sum of the light shift caused by the higher order sidebands (See Appendix).

The density matrix element ρ_{33} is the population of the excited state and it is proportional to the fluorescence intensity. When the atoms fall into the dark state, the fluorescence has the smallest value. Therefore, we investigated the ρ_{33} for calculating the light shift. Figure 3 shows the ρ_{33} as a function of the Raman detuning Δ_0 using Eq. (2), including Eq. (5). We can see that the line shape of the Ramsey-CPT fringe can be calculated in Fig. 3 (a). Figure 3 (b) shows the center part fringe of Ramsey-CPT. The solid line is calculated using Eq. (5) and the dotted line is calculated without using Eq. (5). The Ramsey fringe is a slightly asymmetric resonance with respect to the Raman detuning. It is clearly seen that the minimum value of the ρ_{33} calculated using Eq. (5) is shifted.

III. EXPERIMENTAL SETUP

The experimental setup is shown in Fig. 4. The measurement system is based on the previous Ramsey-CPT observation system [13].

We used a single-mode VCSEL fabricated by Ricoh Company, Ltd. to simultaneously excite two ground states to the common excited state. The wavelength of the VCSEL to excite ^{133}Cs at the D_1 -line was 895 nm. The VCSEL was driven by a DC injection current using a bias T and was modulated at 4.6 GHz using an analog signal generator to generate the first order sidebands around the laser carrier.

The light intensity was modulated for the pulse excitation by using the acousto-optical modulator (AOM). The AOM has a nominal rise and fall time of 65 ns. The total light intensity incident on the gas cell is adjusted by the control voltage of the AOM and is calibrated by the optical power meter.

A Pyrex gas cell containing a mixture of ^{133}Cs atoms and Ne buffer gas at a pressure of 4.0 kPa was used. The gas cell was cylindrical; it had a diameter of 20 mm and optical length of 22.5 mm. The gas cell temperature was maintained at 42.0 °C. The gas cell and Helmholtz coil were covered with a magnetic shield to prevent the external magnetic field from affecting the magnetic field inside the cell. The internal magnetic field of the gas cell was created by the Helmholtz coil. The axis of a 10- μT magnetic field was set to be parallel to the direction of the laser light (C-axis direction).

IV. RESULTS

A. The light shift as a function of the light intensity

Figure 5 (a) shows the calculated light shift as a function of the intensity under pulse excitation. The natural linewidth without buffer gas is $2\pi \times 4.575$ MHz [18], it was used as the emission rate in our calculation. In addition, the AM and FM modulation indexes were set at 0.2 and 1.832, respectively. The calculated slope of the light shift under continuous excitation was 0.174 Hz/ $(\mu\text{W}/\text{cm}^2)$, and the light shift under continuous excitation was proportional to the light intensity within all ranges of light intensity. The light shift under pulse excitation increases with the increase in light intensity. We can see that the light shift under pulse excitation was significantly less than that under continuous excitation. In addition, an important finding here is that the light shift under pulse excitation was nonlinear with regard to the light intensity. Under a small light intensity (< 100 $\mu\text{W}/\text{cm}^2$), the light shift was non-linearly to the light intensity, and the slope of the light shift decreased with the increase in light intensity. The maximum differential light shift value was estimated at 89.1 mHz/ $(\mu\text{W}/\text{cm}^2)$ with the absence of light intensity. Since the maximum differential value under pulse excitation is less than that under continuous excitation, it is understood that pulse excitation enables us to obtain less frequency sensitivity to the light intensity compared to that with continuous excitation. The light shift linearly increases with the increase in light intensity in the light intensity range over 100 $\mu\text{W}/\text{cm}^2$. The solid line is the fitting curve of the light shift in the intensity range from 100 to 1000 $\mu\text{W}/\text{cm}^2$. The slope of the light shift is 3.44 mHz/ $(\mu\text{W}/\text{cm}^2)$ under pulse excitation. A comparison with the slope of the light shift under continuous excitation (0.174 Hz/ $(\mu\text{W}/\text{cm}^2)$) showed that the light shift dependent on the intensity under pulse excitation is one fiftieth smaller than that under continuous excitation. Since the slope of the light shift under pulse excitation for a large light intensity is significantly smaller than that for a small light intensity, in order to reduce the sensitivity of the light shift it is necessary to excite the atoms using a large light intensity. The same qualitative tendency is also proven by the experimental results (Fig. 5 (b)). However, the slope of the light shift with an intensity over 400 $\mu\text{W}/\text{cm}^2$ is four times larger than that of the calculation. This is presumably because the sideband distribution is different from that shown in the Appendix, and the actual emission rate is greater than the

natural linewidth considerably, since Ne buffer gas was contained in the gas cell.

B. The light shift as a function of observation timing

Figure 6 (a) shows the calculated light shift as a function of the observation timing τ_o under different light intensities. The natural linewidth was also used as the emission rate in our calculation. The AM and FM modulation indexes that were set at 0.2 and 1.832, respectively. In the small range of observation timing ($< 100 \mu\text{s}$), the light shift linearly increases with the increase in observation timing τ_o . The slope of the light shift to τ_o increases with the increase in light intensity. Therefore, we found that when a shorter τ_o is set, a smaller light shift can be obtained, and the light shift is approximately proportional to the observation timing τ_o for a small light intensity ($100 \mu\text{W}/\text{cm}^2$). In contrast, for a large light intensity, the light shift non-linearly increases with the increase in observation timing. In particular, for the large range of observation timing ($> 400 \mu\text{s}$), the light shifts are saturated and obtained constant values regardless of the observation timing τ_o variance. Since the saturated light shift is almost equal to the light shift under continuous excitation, we found that the atoms fall into a dark state under continuous excitation.

The time that the light shift saturates is defined as τ_s . We found that the saturation time τ_s decreases with the increase in light intensity. Since the saturation state is the dark state under continuous excitation, the atoms more quickly fall into the dark state for the larger light intensity.

Figure 6 (b) shows the measured light shift as a function of the observation timing τ_o under different light intensities. The experimental results show the same tendency as the calculation results. However, from a quantitative perspective, the difference between the experimental and calculation results occurs in the light shifts and the saturation time τ_s . One of the reasons is that the light shift depends on the emission rate of the excited state and the sideband distribution. Therefore, using the appropriate emission rate and modulation indexes will enable for a precise estimation of the light shift.

V. CONCLUSION

We theoretically and experimentally investigated the light shift of the $6^2S_{1/2}$ ($F = 3 \leftrightarrow 4$) transition frequency in ^{133}Cs under pulse excitation. The light shift in Ramsey-CPT is calculated based on the density matrix analysis. We also showed the experimental results when using a ^{133}Cs gas cell and the D₁-line VCSEL. From the theoretical results of the light shift as a function of total light intensity, we found that the slope of the light shift under pulse excitation is significantly 50 times lower than that under continuous excitation. In addition, the light shift has a non-linear dependency at a small intensity. The light shift as a function of the observation timing is also shown. The light shift under pulse excitation is dependent on the observation timing and increases with the increase in observation timing. An observation during an early time setting showed that the shift is small. From these results, there is a good agreement between the calculation and experiment proving there is the dependence of the light shift on various pulsed laser parameters. Therefore, the analysis method provides us with a precise estimation of the light shift under pulse excitation.

VI. APPENDIX

In this appendix, we show the calculation method of the light shifts of two ground states, LS_1 and LS_2 , under continuous excitation. The light shift contains the frequency shift taking into account the higher order sidebands emitted by the VCSEL.

The light shift between the ground and excited states can be calculated as [19]

$$LS = \frac{1}{4} \frac{\Omega^2 \Delta}{\Delta^2 + \Gamma^2/4}. \quad (6)$$

where Ω is the Rabi frequency, Δ is the detuning from the absorption line, and Γ is the total emission rate. The VCSEL is generally used as the light source for the CPT atomic clocks and the injection current of the VCSEL is modulated by a RF generator in order to generate the two coherent laser beams. However, the higher order sidebands are generated together by the modulation. The higher order sidebands are located near the absorption line and contribute to the light shifts. Therefore, the light shift depends on the modulation depth of VCSEL.

In the case of simultaneous frequency and amplitude modulation, the electric field irradiated by the VCSEL modulated by the RF generator is given as [20]

$$E(t) = E_0(1 + M \sin(\omega_m t + \varphi)) \cdot \exp(i(\omega_0 t + \beta \sin \omega_m t)), \quad (7)$$

where ω_0 is the carrier and ω_m is the modulation frequency. M is the amplitude-modulation (AM) index and β is the frequency modulation (FM) index. E_0 is the electric field strength and φ is the phase between the AM and FM.

From Eq. (7), the laser intensity is calculated using

$$I(t) = \frac{\varepsilon_0 c}{2} E(t) \cdot E^*(t). \quad (8)$$

In the frequency domain, the n -th order sideband intensity $I(n)$ that is contained within $\omega_0 + n\omega_m$ is

$$I(n) = \frac{\varepsilon_0 c E_0^2}{2} \left\{ J_n^2(\beta) + M J_n(\beta) \{ J_{n-1}(\beta) + J_{n+1}(\beta) \} \sin \varphi + \frac{M^2}{4} \{ J_{n-1}^2(\beta) + J_{n+1}^2(\beta) \} - \frac{M^2}{2} J_{n-1}(\beta) J_{n+1}(\beta) \cos 2\varphi \right\}, \quad (9)$$

where $J_n(\beta)$ is the n th-order Bessel functions.

From Eq. (9), the electric field of the n -th order sideband is calculated as

$$E(n) = \sqrt{\frac{2I(n)}{\varepsilon_0 c}}. \quad (10)$$

In the $^{133}\text{Cs-D}_1$ line, the Rabi frequency of each sideband is given as

$$\begin{aligned} \Omega_{ij}(n) &= \frac{\langle i | \hat{\mu} \cdot E(n) | j \rangle}{\hbar} \\ &= \frac{E(n)}{\hbar} \langle i | e_q \hat{r} | j \rangle = \sqrt{\frac{2I(n)}{\varepsilon_0 c \hbar^2}} \langle i | e_q \hat{r} | j \rangle. \end{aligned} \quad (11)$$

Here, $|i\rangle$ is the ground state $6^2\text{S}_{1/2}$ and $|j\rangle$ is the excited state of $6^2\text{P}_{1/2}$. In particular, since $n = +1$ and -1 sidebands are components exciting two ground states, Ω_p and Ω_c correspond to $\Omega_{34'}$ and $\Omega_{44'}$.

Figure 7 shows the histogram of the intensity normalized by the total light intensity in the n order range from -5 to 5 . The AM modulation index is set at 0.2 and the FM modulation index β is set at 1.832 to maximize the intensity ratio of the first sidebands. We found that the higher order sidebands are generated together with the two first sidebands,

and the sideband intensity decreases with the increase in the order n . In addition, since the higher order sideband's detuning from the absorption line increases with the increase in the n order, the influence on the light shift is small with the increase in the n order. Therefore, this enables us to ignore the light shift by using higher order sidebands over 4 ($|n| > 3$).

The detunings of the n -th order sideband are given as

$$\Delta_{ij}(n) = \begin{cases} \Delta_{44'}(n) = \delta_c + \frac{f_S}{2}(n+1) \\ \Delta_{43'}(n) = \Delta_{44'}(n) + f_P \\ \Delta_{34'}(n) = \delta_p + \frac{f_S}{2}(n-1) \\ \Delta_{33'}(n) = \Delta_{34'}(n) + f_P \end{cases}. \quad (12)$$

Here, f_S is the frequency difference between the two ground states of the $6^2S_{1/2}$ ($F = 3 \leftrightarrow 4$). f_P is the frequency difference between the two excited states of the $6^2P_{1/2}$ ($F' = 3 \leftrightarrow 4$).

From Eqs. (11) and (12), the light shifts LS_1 and LS_2 of the two ground states can be calculated by using Eq. (13).

$$\begin{aligned} LS_1 &= \sum_{n=-3}^3 \frac{1}{4} \frac{\Omega_{34'}^2(n) \cdot \Delta_{34'}(n)}{\Delta_{34'}^2(n) + \Gamma_{4'}^2/4} + \frac{1}{4} \frac{\Omega_{33'}^2(n) \cdot \Delta_{33'}(n)}{\Delta_{33'}^2(n) + \Gamma_{3'}^2/4} \\ LS_2 &= \sum_{n=-3}^3 \frac{1}{4} \frac{\Omega_{44'}^2(n) \cdot \Delta_{44'}(n)}{\Delta_{44'}^2(n) + \Gamma_{4'}^2/4} + \frac{1}{4} \frac{\Omega_{43'}^2(n) \cdot \Delta_{43'}(n)}{\Delta_{43'}^2(n) + \Gamma_{3'}^2/4} \end{aligned} \quad (13)$$

We can obtain the light shift under a continuous wave by using modulated VCSEL.

$$LS_{12} = LS_2 - LS_1 \quad (14)$$

Figure 8 shows the light shift as a function of the total light intensity. The light shift linearly increases with the increase in total light intensity.

-
- [1] S. Knappe, L. Liew, V. Shah, P. Schwindt, J. Moreland, L. Hollberg, and J. Kitching, Appl. Phy. Lett. **85**, 1460 (2004).
[2] J. R. Vig, IEEE Trans. Ultra. Ferr. Freq. Control **40**, 522 (1993).

- [3] J. Vanier, M. Levine, S. Kendig, D. Janssen, C. Everson, and M. Delaney, *IEEE Trans. Instrum. Meas.* **54**, 2531 (2005).
- [4] M. Arditi, and T. R. Carver, *Phys. Rev.* **124**, 800 (1961).
- [5] J. Vanier, and C. Audoin, *The Quantum Physics of Atomic Frequency Standards*, (A. Hilger, Bristol, 1989).
- [6] S. Knappe, R. Wynands, J. Kitching, H. G. Robinson, and L. Hollberg, *J. Opt. Soc. Am. B.* **18**, 1545 (2001).
- [7] O. Kozlova, R. Boudot, S. Guerandel, and E. de Clercq, *IEEE Trans. Instrum. Means.* **60**, 2262 (2011).
- [8] M. Pellaton, C. Affolderbach, Y. Petremand, N. de Rooig, and G. Mileti, *Phys. Scr.*, T149, 014013 (2012).
- [9] C. Affolderbach, C. Andreeva, S. Cartaleva, T. Karaulanov, G. Mileti, and D. Slavov, *Appl. Phys. B.* **80**, 841 (2005).
- [10] B. H. McGuyer, Y-Y. Jau, and Happer, *Appl. Phys. Lett.* **94**, 251110 (2009).
- [11] D. Miletic, C. Affolderbach, M. Hasegawa, R. Boudot, C. Gorecki, and G. Mileti, *Appl. Phys. B.* **109**, 89 (2012).
- [12] N. Castagna, R. Boudot, S. Gurandel, E. De Clercq, N. Dimarcq, and A. Clairon, *IEEE Trans. Ultrason. Ferroelectr. Freq. Control* **56**, 246 (2009).
- [13] Y. Yano, and S. Goka, *Jpn. J. Appl. Phys.* **51**, 122401 (2012).
- [14] I. Yoshida, N. Hayashi, K. Fujita, S. Taniguchi, Y. Hoshina, and M. Mitsunaga, *Phys. Rev. A.* **87**, 023836 (2013).
- [15] J. M. Danet, M. Lours, P. Yun, S. Guerandel, and E. de Clercq, *Proceeding "2013 joint UFFC, EFTF and PFM Symposium"*, 586 (2013).
- [16] J. Vanier, A. Godone, and F. Levi, *Phys. Rev. A.* **58**, 2345 (1998).
- [17] T. Zanon, S. Tremine, S. Guerandel, E. de Clercq, D. Holleville, N. Dimarcq, and A. Clairon, *IEEE Trans. Instrum. Meas.* **54**, 776 (2005).
- [18] D. A. Steck. (2010, Dec.). Cesium D line data. [Online]. Available: <http://steck.us/alkalidata>
- [19] F. Levi, A. Godone, and J. Vanier, *IEEE Trans. Ultrason. Ferroelectr. Freq. Control* **47**, 466 (2000).
- [20] W. Lenth, *Opt. Lett.* **8**, 575 (1983).

VII. FIGURES

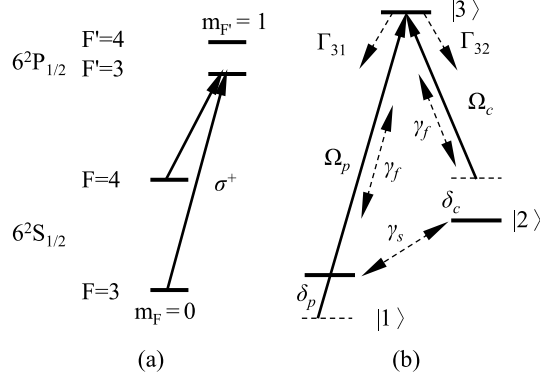


FIG. 1: (a) Excitation scheme with left circular polarized (σ^+) light field on D₁-line of Cs. (b) Closed Λ -type three level model used to calculate CPT phenomenon: δ_p and δ_c are detunings of probe laser and coupling laser, and Ω_p and Ω_c are Rabi frequencies. Γ_{31} and Γ_{32} are the relaxation terms between an excited state and the two ground states. γ_f is the decoherence rate between the excited state and ground states and γ_s is the decoherence rate between the two ground states

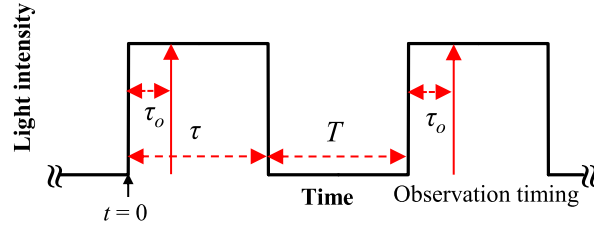
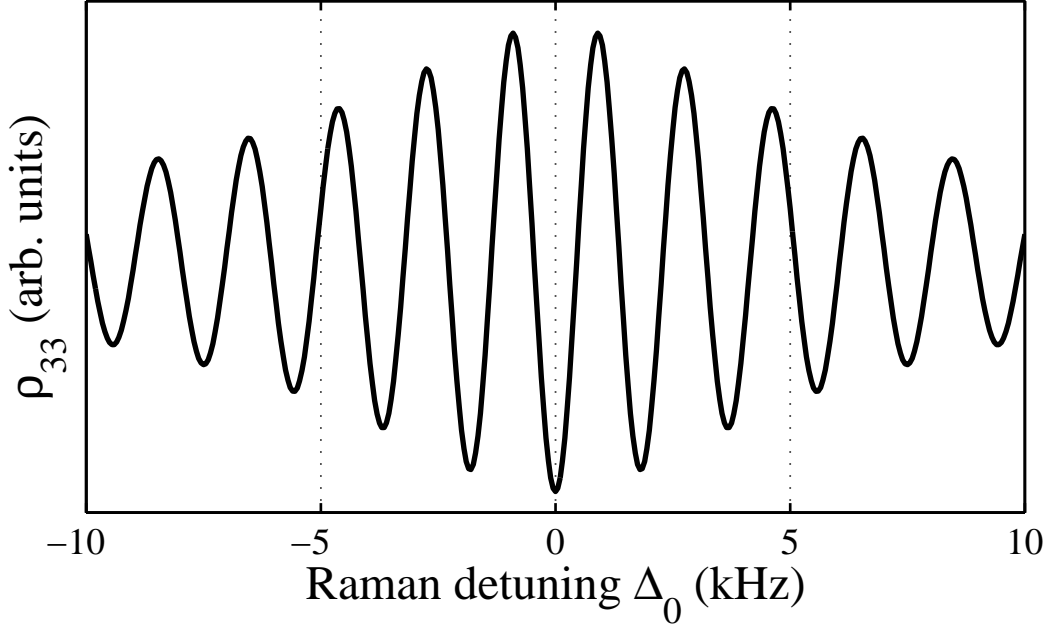
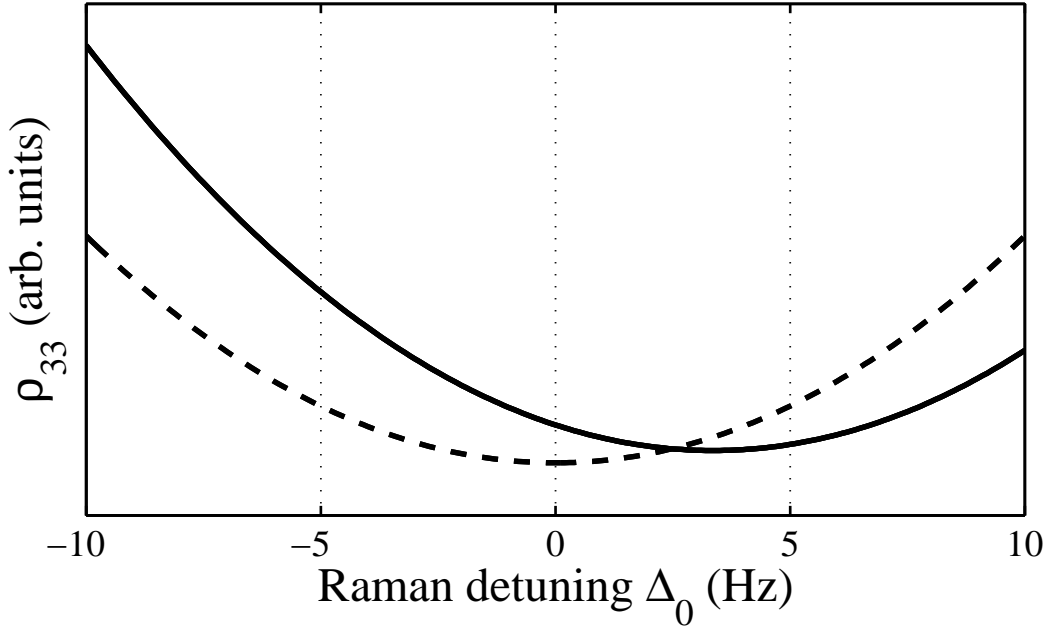


FIG. 2: Ramsey pulse sequence: τ is excite time, T is free evolution time, and τ_o is observation timing of resonance signal.



(a)



(b)

FIG. 3: (a) Line shape of ρ_{33} in detuning range from -10 to 10 kHz. (b) Line shape of ρ_{33} in detuning range from -10 to 10 Hz, solid line is calculated using Eq. (5), and dotted line is calculated without using Eq. (5). τ and T are set at $500 \mu\text{s}$ and the observation timing τ_o is $10 \mu\text{s}$. The emission rate is $2\pi \times 4.575 \text{ MHz}$. The total light intensity is $200 \mu\text{W}/\text{cm}^2$ and the AM and FM modulation index of VCSEL are 0.2 and 1.832, respectively.

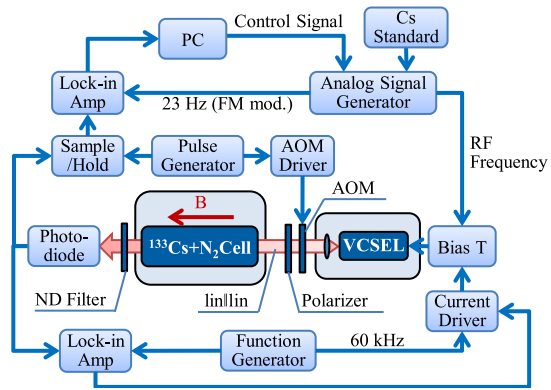
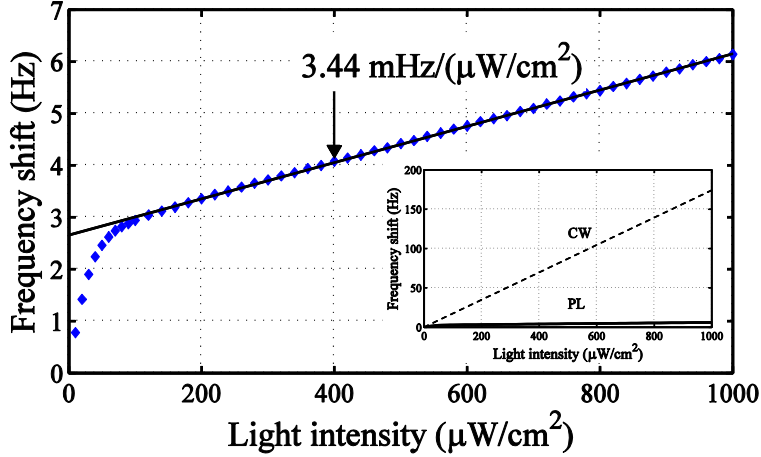
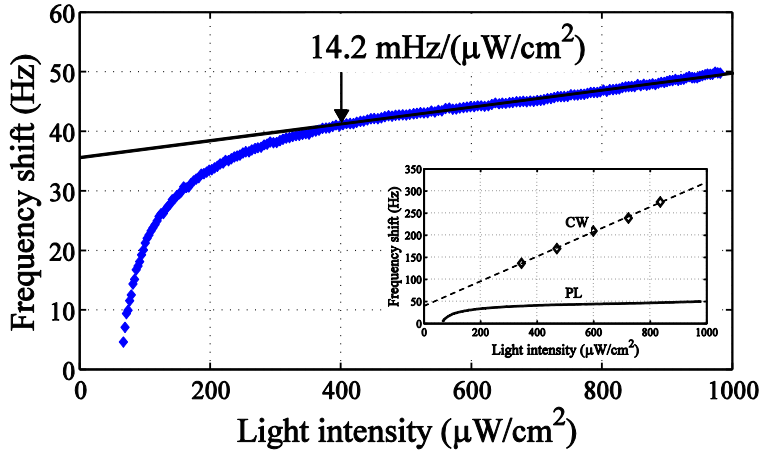


FIG. 4: Experimental setup.

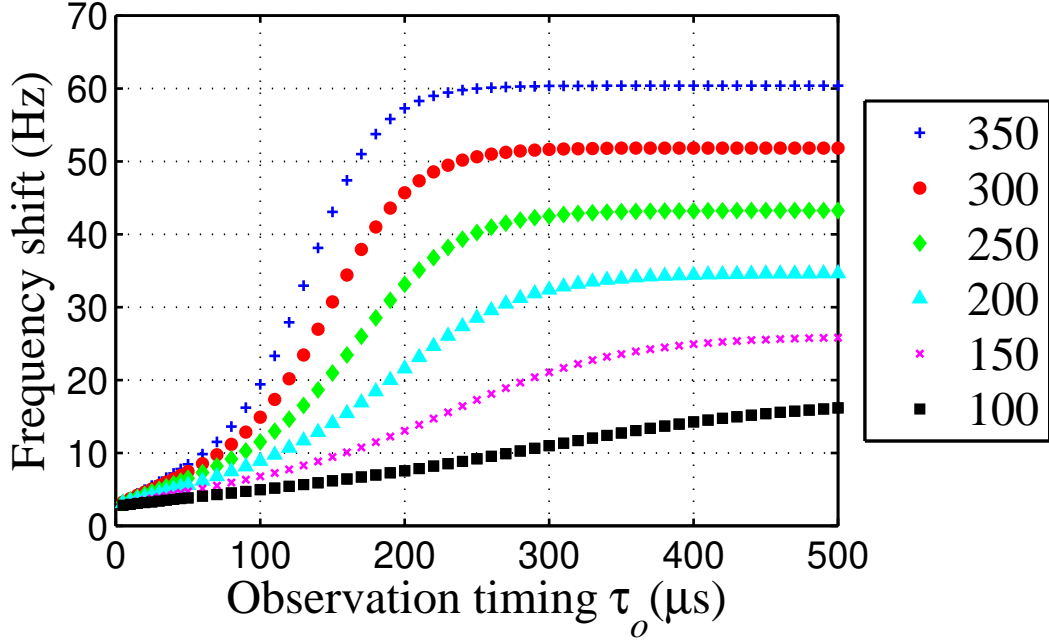


(a)

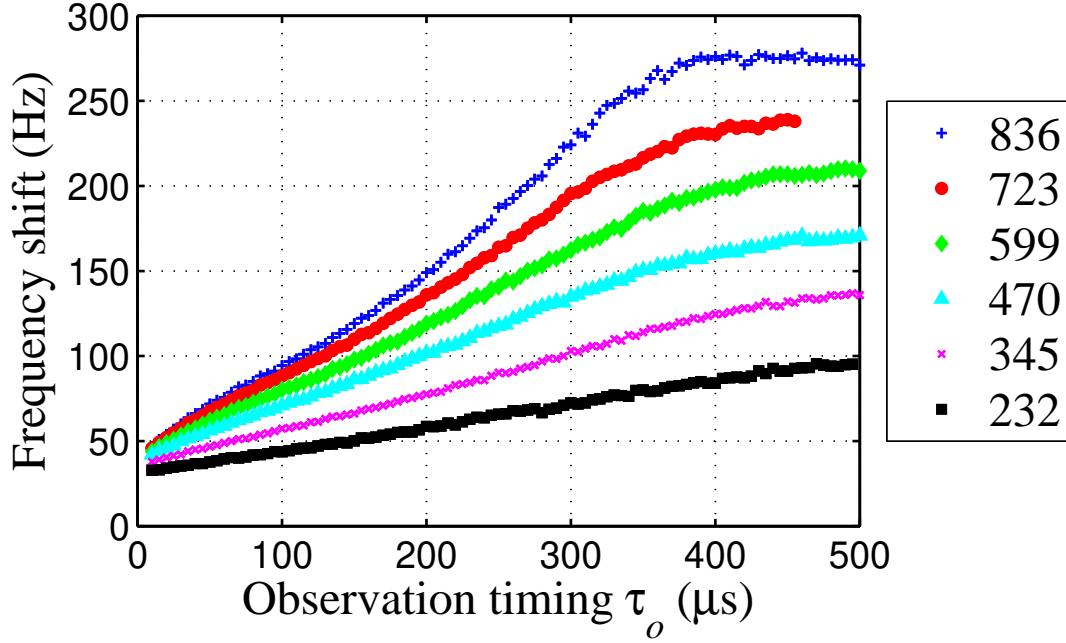


(b)

FIG. 5: (a) Calculated light shift as function of total light intensity under Ramsey excitation: Excitation duration time τ is $500 \mu\text{s}$ and free evolution time T is $500 \mu\text{s}$. The observation timing τ_o is $10 \mu\text{s}$. (b) Measured light shift as function of total light intensity under Ramsey excitation: Resonance frequency at which light intensity is zero is 4.592325 GHz shifted from unperturbed hyperfine transition frequency by 18 kHz . The frequency shift is caused by the buffer gas shift. At a weak light intensity ($<65 \mu\text{W}/\text{cm}^2$), the resonance amplitude is so small that we cannot measure the light shift. The slope of the light shift under continuous excitation is $0.280 \text{ Hz}/(\mu\text{W}/\text{cm}^2)$. The light shift with CW and PL excitation are plotted in the insert, where the dotted line is the light shift under continuous excitation and the solid line is the light shift under pulse excitation.



(a)



(b)

FIG. 6: (a) Calculated light shift as function of observation timing τ_o under different light intensities whose units are $\mu\text{W}/\text{cm}^2$. (b) Measured light shift as function of observation timing τ_o under different light intensities whose units are $\mu\text{W}/\text{cm}^2$. The excitation duration time τ is 500 μs and the free evolution time T is 500 μs .

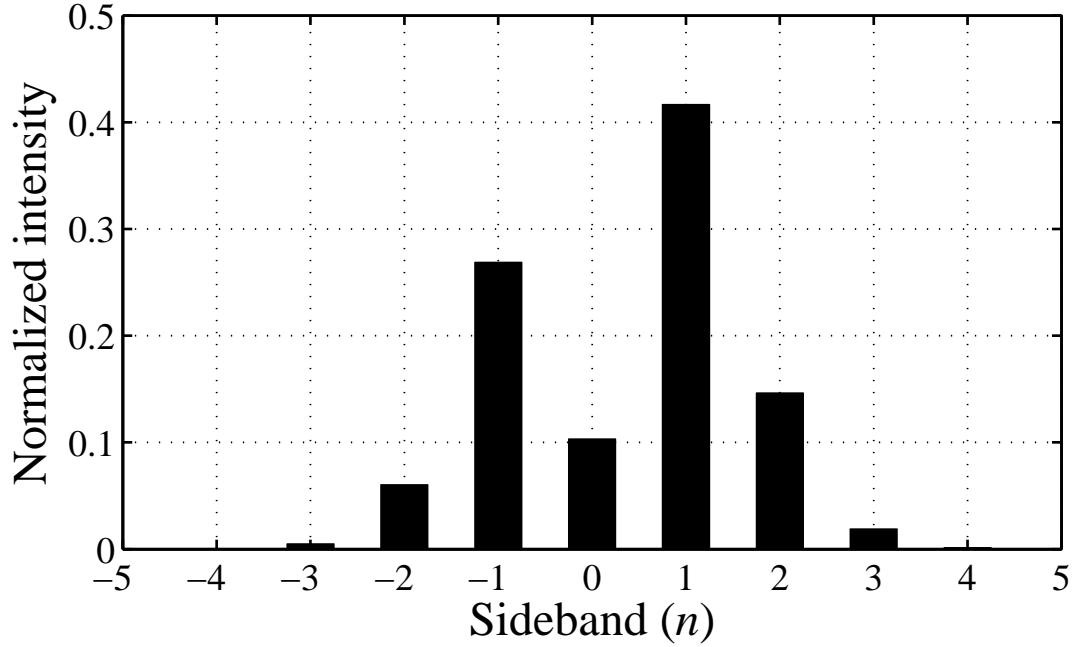


FIG. 7: Histogram of each order light intensity normalized by total light intensity: $M = 0.2$, $\beta = 1.832$ and $\varphi = \pi/2$.

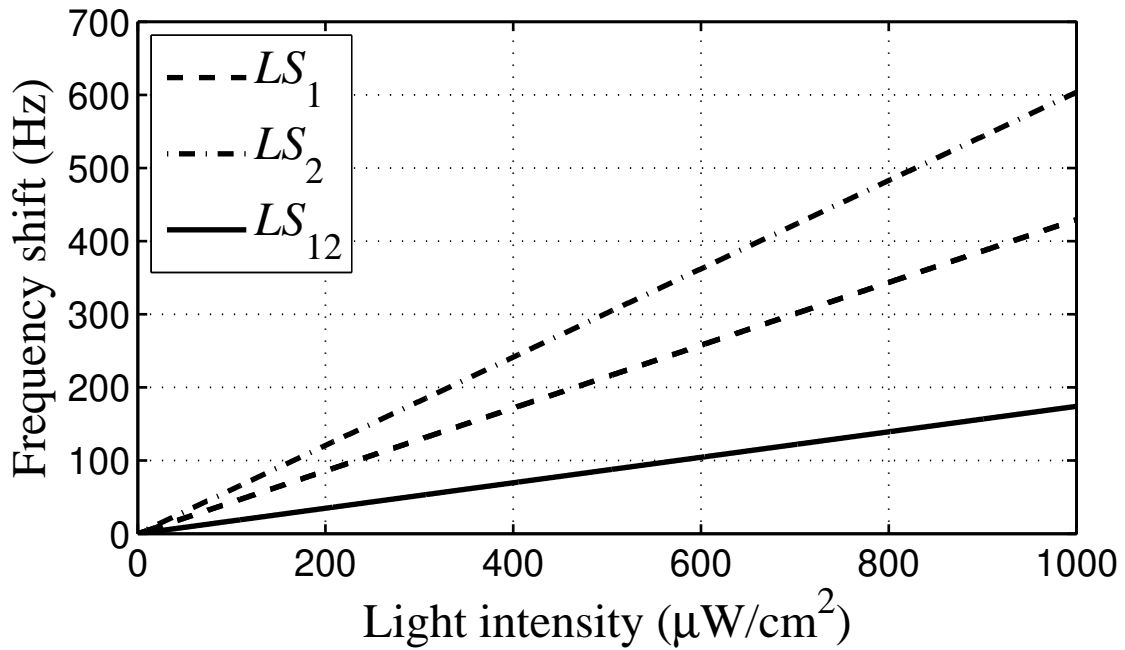


FIG. 8: Light shift as function of total light intensity.